# Photochemistry of $Os(dmpe)_2H_2$: Matrix, Transient Solution, and NMR Studies of 16-Electron $Os(dmpe)_2$ ($dmpe = Me_2PCH_2CH_2PMe_2$)

Maria-Carmen Nicasio, Robin N. Perutz,* and Aysin Tekkaya

*Department of Chemistry, University of York, York, YO10 5DD, U.K.*

*Received July 20, 1998*

The complex $Os(dmpe)_2H_2$ ($dmpe = Me_2PCH_2CH_2PMe_2$) was synthesized by reaction of *trans*-$Os(dmpe)_2Cl_2$ with sodium under hydrogen and was shown to consist of cis and trans isomers in a ratio of ca. 60:1. UV irradiation in argon and methane matrices yielded $Os(dmpe)_2$ with a characteristic multiband UV−vis spectrum; the lowest energy transition occurs close to 800 nm. In CO-doped matrices, $Os(dmpe)_2(CO)$ was generated. Laser flash photolysis experiments (266 nm excitation) demonstrated that the same species was produced in cyclohexane solutions of $Os(dmpe)_2H_2$ at room temperature. The initial photoproduct, $Os(dmpe)_2$, is formed within 60 ns of the laser flash. This species reacts with hydrogen and with CO with rate constants exceeding $10^9$ $dm^3$ $mol^{-1}$ $s^{-1}$, indicating that there is essentially no barrier to its reaction with these substrates. Rate constants for reaction with ethene, triethylsilane, and nitrogen are all close to $10^8$ $dm^3$ $mol^{-1}$ $s^{-1}$. Comparison of the UV−vis spectrum of $Os(dmpe)_2$ with $Ru^0$, $Rh^+$, and $Ir^+$ analogues indicates that $Os(dmpe)_2$ has a structure close to square planar (local $D_{2h}$ symmetry). The products of photochemical reaction of $Os(dmpe)_2H_2$ in solution were also studied by NMR spectroscopy. Reaction with benzene yields *cis*-$Os(dmpe)_2(Ph)H$, while reaction with ethene yields *cis*- and *trans*-$Os(dmpe)_2(CH{=}CH_2)H$.

## Introduction

The familiarity of $d^8$-square planar compounds of $Rh^I$, $Ir^I$, $Pd^{II}$, and $Pt^{II}$ contrasts with the high reactivity of their $Ru^0$ and $Os^0$ analogues. Isolable examples of four-coordinate $Ru^0$ and $Os^0$ complexes can be found among sterically hindered complexes such as Werner's metal nitrosyls and Caulton's recent dicarbonyl complexes.[1,2] Simpler examples are known only as transient intermediates or matrix-isolated species.[3−9] Weitz et al. have observed $Ru(CO)_4$ and $Os(CO)_4$ by time-resolved IR spectroscopy, but have not been able to prove their structures experimentally.[3]

We have used the photosensitivity of metal dihydride and related complexes as an entry to the study of the structure and reactivity of species of the type $MP_4$, $MP_3(CO)$, and $MP_2(CO)_2$ (P = phosphine).[4−9] We have already reported on the contrasting reactivity and UV−vis spectra of $Ru(dmpe)_2$ and $Fe(dmpe)_2$ ($dmpe = Me_2PCH_2CH_2PMe_2$) and have deduced that the structure of $Ru(dmpe)_2$ is close to square planar, whereas $Fe(dmpe)_2$ probably has a butterfly structure.[4,5] The case for the square planar structure of the $RuP_4$ skeleton is reinforced by studies of $Ru(depe)_2$ and $Ru(dppe)_2$ ($depe = Et_2PCH_2CH_2PEt_2$, $dppe = Ph_2PCH_2CH_2PPh_2$). Each of these $Ru^0$ species exhibits a complex multiband UV−vis spectrum with three absorption maxima between ca. 800 and 400 nm.[6] In contrast, $Fe(dmpe)_2$ shows only one maximum, which is located at 355 nm. We have also shown that the replacement of two phosphine ligands by carbonyl groups changes the structure to a trigonal bipyramid in which the fifth position is occupied by the matrix species or solvent: $Ru(CO)_2(PMe_3)_2S$ and $Ru(CO)_2(dmpe)S$.[7] Parallel investigations of $M(PP_3)$ ($PP_3 = P(CH_2CH_2PPh_2)_3$) have shown dramatic alterations in the spectrum as a result of the constraints of a tetradentate phosphine, which has the added possibility of an agostic interaction with the phenyl group.[8] Theoretical investigations of $Ru(PH_3)_4$ by density functional methods have predicted a $D_{2d}$ structure close to the square planar limit (P−Ru−P = 159°). The calculations located the $d_{z^2}-p_z$ transition close to the experimental absorption maximum of $Ru(dmpe)_2$ at ca. 725 nm and predicted a large shift in $\lambda_{max}$ between $Ru(PH_3)_4$ and $[Rh(PH_3)_4]^+$, as observed in the dmpe analogues.[10]

---

[1] Werner, H.; Flügel, R.; Windmüller, B.; Michenfelder, A.; Wolf, J. *Organometallics* **1995**, *14*, 612. Flügel, R.; Windmüller, B.; Gevert, O.; Werner, H. *Chem. Ber.* **1996**, *129*, 1007.

[2] De C. T. Carrondo, M. A. A. F.; Chaudret, B. N.; Cole-Hamilton, D. J.; Skapski, A. C.; Wilkinson, G. *J. Chem. Soc., Chem. Commun.* **1978**, 463. Chaudret, B. N.; Cole-Hamilton, D. J.; Wilkinson, G. *J. Chem. Soc., Dalton Trans.* **1978**, 1739. Ogasawara, M.; Macgregor, S. A.; Streib, W. E.; Folting, K.; Eisenstein O.; Caulton, K. G. *J. Am. Chem. Soc.* **1995**, *117*, 8869; *J. Am. Chem. Soc.* **1996**, *118*, 10189.

[3] Bogdan, P. L.; Weitz, E. *J. Am. Chem. Soc.* **1989**, *111*, 3163; **1990**, *112*, 639.

[4] Hall, C.; Jones, W. D.; Mawby, R. J.; Osman, R.; Perutz, R. N.; Whittlesey, M. K. *J. Am. Chem. Soc.* **1992**, *114*, 7425.

[5] Whittlesey, M. K.; Mawby, R. J.; Osman, R.; Perutz, R. N.; Field, L. D.; Wilkinson, M. P.; George, M. W. *J. Am. Chem. Soc.* **1993**, *115*, 8627.

[6] Cronin, L.; Nicasio, M. C.; Perutz, R. N.; Peters, R. G.; Roddick, D. M.; Whittlesey, M. K. *J. Am. Chem. Soc.* **1995**, *117*, 10047.

[7] Mawby, R. J.; Perutz, R. N.; Whittlesey, M. K. *Organometallics* **1995**, *14*, 3268. Whittlesey, M. K.; Perutz, R. N.; Virrels, I. G.; George, M. W. *Organometallics* **1997**, *16*, 268.

[8] Osman, R.; Pattison, D. I.; Perutz, R. N.; Bianchini, C.; Casares, J. A.; Peruzzini, M. *J. Am. Chem. Soc.* **1997**, *119*, 8459.

[9] Colombo, M.; George, M. W.; Moore, J. N.; Pattison, D. I.; Perutz, R. N.; Virrells, I. G.; Ye, T. Q. *J Chem Soc., Dalton Trans.* **1997**, 2857.

[10] Macgregor, S. A.; Cronin, L.; Eisenstein, O.; Whittlesey, M. K.; Perutz, R. N. *J. Chem. Soc., Dalton Trans.* **1998**, 291.

10.1021/om9806141 CCC: $15.00
Publication on Web 11/19/1998

**Table 1. $^1H$ (Hydride Only) and $^{31}P\{^1H\}$ NMR Spectroscopic Data in $C_6D_6$ at 25 °C**

| | $^1H$ NMR, hydride | | $^{31}P\{^1H\}$ NMR | |
|---|---|---|---|---|
| compound | $\delta$ | mult, $J$/Hz | $\delta$ | mult, $J$/Hz |
| *cis*-Os(dmpe)$_2$H$_2$ | −11.10 | $[AMX]_2$,[a] $J_{MX} = J_{M'X'} = -19$, $J_{MX'} = J_{M'X} = +56$, $J_{XX'} = \pm 6$, $J_{AX'} = J_{A'X} = -22$, $J_{A'X'} = J_{AX} = -20$, $J_{MM'} = 2$, $J_{AM'} = J_{A'M} = -12$, $J_{AM} = J_{A'M'} = -10$, $J_{AA'} = +270$ | 1.49<br>7.56 | t, 11.1<br>t, 11.1 |
| *cis*-Os(dmpe)$_2$(H)(Ph)[b] | −9.33 | dq, 71.4, 20.6 | $\delta_A = 7.8$, $\delta_B = 3.0$, $\delta_M = -5.6$, $\delta_Q = -6.1$ | ABMQ, $J_{AB} = 264$, $J_{AM} = 18$, $J_{AQ} = 3$, $J_{BM} = 13$, $J_{BQ} = 4$, $J_{MQ} = 4$ |
| *cis*-Os(dmpe)$_2$(H)(C$_2$H$_3$)[b] | −9.47 | dq, 68.3, 19.7 | $\delta_A = 7.50$, $\delta_B = 4.19$, $\delta_M = -0.84$, $\delta_Q = -3.43$ | $J_{AB} = 263.2$, $J_{AM} = 5.0$, $J_{AQ} = 14.5$, $J_{BM} = 17.0$, $J_{BQ} = 3.0$, $J_{MQ} = 5$ |
| *trans*-Os(dmpe)$_2$(H)(C$_2$H$_3$) | −10.1 | q, 20.0 | 9.58 | s |
| *trans*-Os(dmpe)$_2$(H)(SiEt$_3$) | −10.81 | br t, ~6 | −5.1 | s |
| *cis*-Os(dmpe)$_2$(H)(SiEt$_3$)[b] | −11.26 | dq, 51.0, 18.4 | $\delta_A = 0.5$, $\delta_B = 0.4$, $\delta_M = -2.4$, $\delta_Q = -3.5$ | ABMQ, $J_{AB} = 260$, $J_{AM} = 12$, $J_{AQ} = 18$, $J_{BM} = 13$, $J_{BQ} = 15$, $J_{MQ} = 9$ |

[a] For atom labels, see text diagram. Coupling constants determined by simulation. The simulation is unaffected by permutation of A and A′ or by the sign of $J_{XX'}$. [b] A and B refer to mutually trans P nuclei; more specific assignments of $^{31}P$ resonances have not been made.

The structural complexity of the $MP_4$ and $MP_2(CO)_2$ complexes parallels large variations in the kinetics of reaction. Alteration of the metal and phosphine causes major changes both in the magnitude of the rate constants and in their relative values. The rates of reaction toward $H_2$, CO, $Et_3SiH$, and benzene provide tests of both oxidative addition and ligand attack. Transient Ru(dmpe)$_2$ reacts with $H_2$ and with CO at rates close to the diffusion limit ($>10^9$ dm$^3$ mol$^{-1}$ s$^{-1}$).[4] No reaction with benzene is detected by laser flash photolysis. Replacement of the methyl group by ethyl or phenyl groups reduces the rate constants progressively and in some cases increases the selectivity; for instance, $k(H_2)/k(Et_3SiH)$ increases from ca. 30 for Ru(dmpe)$_2$ to 3600 for Ru(depe)$_2$.[6] On the other hand, the rate constants for reaction of Ru(PP$_3$) with all the above reagents, including benzene, are around $10^6$ dm$^3$ mol$^{-1}$ s$^{-1}$.[8] The reactivity of Os(PP$_3$) toward CO, $Et_3SiH$, and benzene is similar to that of Ru(PP$_3$). However, the rate of reaction with $H_2$ is reduced and C−H activation is observed with the aliphatic C−H bonds of THF and alkanes. The photoreactions of M(PP$_3$)(H$_2$) (M = Ru and Os) with benzene yield the C−H activation products, M(PP$_3$)(Ph)H.[8]

A study of the photochemistry of Os(dmpe)$_2$H$_2$ was essential in order to complete the comparisons of the group 8 metals. Moreover, we anticipated that Os(dmpe)$_2$ would be more reactive than Ru(dmpe)$_2$ with respect to C−H oxidative addition. Whereas Fe(dmpe)$_2$H$_2$ and Ru(dmpe)$_2$H$_2$ were first characterized many years ago,[11] Os(dmpe)$_2$H$_2$ has been mentioned in the literature only once, without details of the synthesis and characterization.[12a] However, related osmium dihydride complexes containing other diphosphines have been fully described.[12b] In this paper, we report the characterization of Os(dmpe)$_2$H$_2$, an investigation of its steady state and transient photochemistry in solution, and its photochemistry in low-temperature matrices. We show that Os(dmpe)$_2$ and Ru(dmpe)$_2$ have a similar reactivity toward hydrogen and carbon monoxide. The UV−vis spectrum of Os(dmpe)$_2$ proves even richer than that of Ru(dmpe)$_2$.

## Results

**Synthesis.** Reaction of *trans*-Os(dmpe)$_2$Cl$_2$ with sodium in THF under 1 atm $H_2$ yielded Os(dmpe)$_2$H$_2$ as a white compound, which was purified by sublimation. The $^{31}P\{^1H\}$ NMR spectrum showed that the product is present in two isomeric forms. The major isomer has cis stereochemistry, as shown by the two triplets at $\delta$ 1.47 and $\delta$ 7.52 with an apparent coupling constant $J_{PP}$ of 11 Hz. A minor singlet resonance observed at $\delta$ 7.74 is assigned to the trans isomer. The $^1H$ NMR spectrum recorded in benzene-$d_6$ showed a complex hydride resonance for the cis isomer at $\delta$ −11.1. Another hydride resonance appeared at $\delta$ −12.86 as a quintet ($J_{PH}$ = 16.8 Hz) which belongs to the trans isomer (1.6% relative to cis isomer). The IR spectrum shows the osmium−hydride stretching band at 1863 cm$^{-1}$ in nujol.

The hydride nuclei form a part of an $[AMX]_2$ spin system in which the two mutually trans phosphorus nuclei become magnetically inequivalent thanks to the links through the carbon backbones. The diagram below indicates our labeling system with the hydride nuclei designated X and X′. Preliminary estimates of the coupling constants for *cis*-Os(dmpe)$_2$H$_2$ were obtained by recording the $^1H$ spectrum with selective $^{31}P$ decoupling. When the P nuclei cis to the hydrides were decoupled, the spin system was simplified to $A_2X_2$; when the P nuclei trans to the hydrides were decoupled, it became an $[MX]_2$ system. Further analysis of the couplings was achieved by computer simulation of the $^1H$ and $^{31}P\{^1H\}$ spectra with the assumption that $^2J_{PH-trans}$ is positive, as has been demonstrated elsewhere (Table 1).[13] Most of the resulting values fit the generalizations that have been established for related

---

(11) Chatt, J.; Davidson, J. M. *J. Chem. Soc.* **1965**, 843. Gerlach, D. H.; Peet, W. G.; Muetterties, E. L. *J. Am. Chem. Soc.* **1972**, *94*, 4545.

(12) (a) Bergamini, P.; Sostero, O.; Traverso, O. *J. Organomet. Chem.* **1986**, *299*, C11. (b) Chatt, J.; Hayter, R. G. *J. Chem. Soc.* **1961**, 2605. Capellani, E. P.; Maltby, P. A.; Morris, R. H.; Schweitzer, C. T.; Steele, M. R. *Inorg. Chem.* **1989**, *28*, 4437. Kelly, A. E.; Jia, G.; Maltby, P. A.; Morris, R. H. *J. Am. Chem. Soc.* **1991**, *113*, 3027.

systems that $^2J_{\mathrm{PH-cis}}$ and $^2J_{\mathrm{PP-cis}}$ are then negative and $^2J_{\mathrm{PP-trans}}$ is positive and that $|^2J_{\mathrm{PH-trans}}| > |^2J_{\mathrm{PH-cis}}|$.[14] One calculated $^2J_{\mathrm{PP-cis}}$ coupling constant is, however, surprisingly small. Very small PP coupling constants have been observed previously in osmium systems.[8,15] The computer simulation certainly does not give a unique solution; indeed the spectrum is unchanged by permutation of the A and A′ phosphorus nuclei.

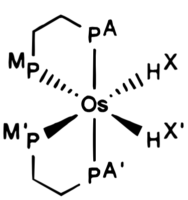

**Matrix Isolation Experiments.** The vapor of *cis*-Os(dmpe)$_2$H$_2$ was co-condensed with argon onto a window at 20 K before cooling the resulting matrix to 12 K for study by IR and UV−vis spectroscopy. The IR spectrum in a methane matrix displayed a group of broad metal hydride stretching bands, centered at 1882 cm$^{-1}$ together with bands due to the dmpe ligand at lower wavenumbers (see Experimental Section). The UV−vis spectrum in the same matrix was broad and featureless.

Broad band UV−vis photolysis ($\lambda > 200$ nm, 15 min) of *cis*-Os(dmpe)$_2$H$_2$ in a CH$_4$ matrix at 12 K resulted in depletion of the $\nu$(OsH) modes of the starting dihydride by ca. 25% (by area) without formation of new bands in this region. In the UV−vis spectrum four prominent bands grew in (438, 493, 584, 640 (sh), 793 nm, Figure 1a (i)). Selective photolysis coincident with *one* of the maxima ($\lambda = 493$ nm interference filter) resulted in depletion of all the UV−vis bands (Figure 1a (ii)) and recovery of precursor to 96% of the original area. The observation that all the UV−vis bands grow in together and are bleached together, even with very selective irradiation, indicates that they belong to the same species.

The behavior of *cis*-Os(dmpe)$_2$H$_2$ in an argon matrix was extremely similar. The IR spectrum after deposition showed a cluster of Os−H stretching bands which decreased in intensity by 25% by area after 30 min photolysis ($\lambda > 200$ nm), rising to 53% depletion after 90 min photolysis (Figure 2; see also Experimental Section). The different components of the IR spectrum in this region decreased at different rates such that photolysis caused a redistribution of intensity to lower wavenumbers. The UV−vis spectrum obtained after irradiation showed the presence of a new species with bands at 447, 497, 596, 650 (sh), and 798 nm (Table 2). Selective photolysis ($\lambda = 493$ nm) for ca. 13 h caused a reduction of the intensity of these bands together with a recovery of the Os−H stretching bands in the IR spectrum to 62% of their original area.

The similarity of the spectra in argon and methane matrices indicates that there is no interaction between the new species and the matrix host, nor reaction with methane. The spectrum of Ru(dmpe)$_2$ closely resembles that observed here and also proved insensitive to the matrix material. In contrast, Ru(CO)$_2$(dmpe) exhibited a much simpler UV−vis spectrum, which was highly sensitive to the matrix material. We therefore assign the photoproduct of *cis*-Os(dmpe)$_2$H$_2$ as Os(dmpe)$_2$ (eq 1):

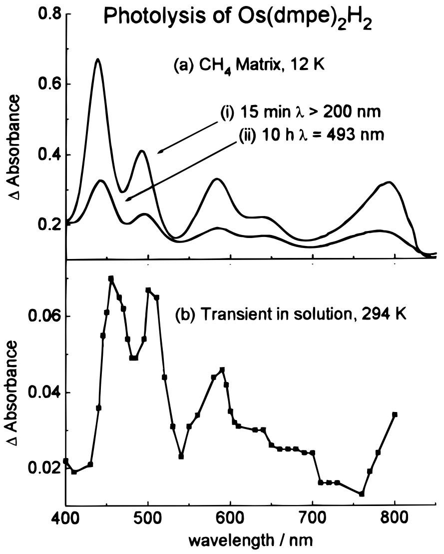

**Figure 1.** (a) UV−vis spectra of Os(dmpe)$_2$H$_2$ in a methane matrix (2 h deposition, sample at 333 K, window at 25 K during deposition, subsequently cooled to 12 K) (i) after initial photolysis of precursor with $\lambda > 200$ nm for 15 min; (ii) after subsequent selective photolysis of the product at $\lambda = 493$ nm for 10 h. (b) Flash kinetic spectrum measured 100 ns after flash photolysis (laser wavelength 266 nm) of a solution of Os(dmpe)$_2$H$_2$ in cyclohexane at 294 K. Note that the precursor shows no absorptions in the region of the spectrum illustrated.

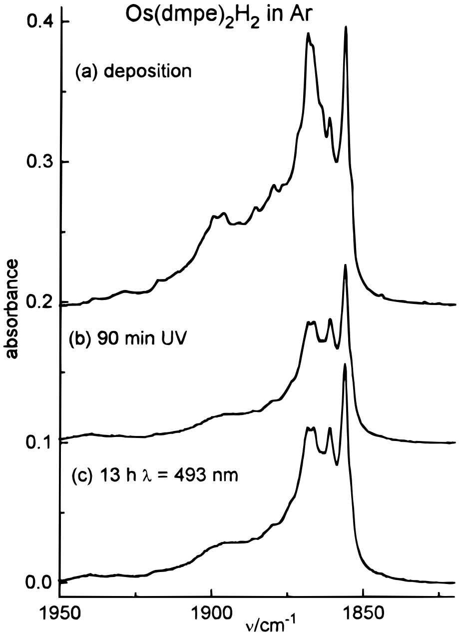

**Figure 2.** IR spectra in Os−H stretching region of Os(dmpe)$_2$H$_2$ in an argon matrix (2 h deposition, sample at 333 K, window at 20 K, subsequently cooled to 12 K) (a) after deposition; (b) after initial photolysis of precursor with $\lambda > 200$ nm for 90 min; (c) after subsequent selective photolysis at $\lambda = 493$ nm for 13 h.

---

[13] Duckett, S. B.; Barlow, G. K.; Partridge, M. G.; Messerle, B. A. *J. Chem. Soc., Dalton Trans.* **1995**, 3427.

[14] Bampos, N.; Field, L. D.; Messerle, B. A. *Organometallics* **1993**, *12*, 2529, and references therein.

[15] Tolman, C. A.; Ittel, S. D.; English, A. D.; Jesson, J. P. *J. Am. Chem. Soc.* **1978**, *100*, 4080.

**Table 2. UV−Vis Absorption Maxima of Os(dmpe)$_2$**

| medium and temp/K | $\lambda_{max}$/nm | | | | |
|---|---|---|---|---|---|
| Ar/12 K[a] | 798 | 650 (sh) | 596 | 497 | 447 |
| $CH_4$/12 K[a] | 793 | 640 (sh) | 584 | 493 | 438 |
| cyclohexane/296 K[b] | ca. 800[c] | 640 (sh) | 590 | 500 | 455 |

[a] ±3 nm. [b] ±5 nm. [c] The spectrum was not recorded beyond 800 nm.

$$cis\text{-Os(dmpe)}_2\text{H}_2 \underset{\text{vis}}{\overset{\text{UV}}{\rightleftharpoons}} \text{Os(dmpe)}_2 + \text{H}_2 \qquad (1)$$

In an argon matrix doped with 2% CO, the Os−H stretching band of *cis*-Os(dmpe)$_2$H$_2$ appeared as a broad asymmetrical feature at 1867 cm$^{-1}$. UV−vis photolysis ($275 < \lambda < 390$ nm, 30 min) generated a new band in the IR spectrum at 1851 cm$^{-1}$, which was assigned to Os(dmpe)$_2$(CO) (compare 1859 cm$^{-1}$ for Ru(dmpe)$_2$(CO)).[4] A much weaker product feature at 1954 cm$^{-1}$ has not been identified. After irradiation for a further hour, other bands appeared at 1843 and 1933 cm$^{-1}$, which were tentatively assigned to Os(dmpe)($\eta^1$-dmpe)(CO)$_2$.[16] When photolysis was continued with visible light ($\lambda >$ 395 nm), production of monocarbonyl complex continued while formation of dicarbonyl complex nearly stopped. Presumably, visible photolysis converts Os(dmpe)$_2$ to Os(dmpe)$_2$(CO). Since the C−O stretching band of the product overlapped severely with the Os−H stretching bands of the precursor, a similar experiment was performed in a 2% $^{13}$CO/Ar matrix. The $\nu_{CO}$ band of Os(dmpe)$_2$($^{13}$CO) was observed at 1808 cm$^{-1}$ well separated from the OsH stretching band of the precursor.

**Flash Photolysis.** The UV−vis spectrum of the white precursor dissolved in cyclohexane displayed a maximum at 204 nm with two shoulders at 218 and 300 nm. The extinction coefficient at 308 nm, the laser wavelength we have usually employed, was insufficient for transient absorption studies. We therefore used a frequency-quadrupled YAG laser with output at 266 nm instead. At this wavelength Os(dmpe)$_2$H$_2$ has an extinction coefficient of 2.75 × 10$^3$ dm$^3$ mol$^{-1}$ cm$^{-1}$. Laser flash photolysis (pulse width ca. 10 ns, pulse energy ca. 8−10 mJ) of cyclohexane solutions of the *cis*-Os(dmpe)$_2$H$_2$ of concentration ca. 10$^{-3}$ mol dm$^{-3}$ under argon at room temperature generated a transient species, monitored at 450 nm, which decayed over 30 $\mu$s with pseudo-first-order kinetics ($k_{obs} = 2.8 \times 10^5$ s$^{-1}$), without returning to the baseline. A similar experiment with heptane under argon yielded a slightly larger rate constant of 6.5 × 10$^5$ s$^{-1}$.

The UV−vis spectrum of the transient species formed upon photolysis in cyclohexane was measured under a partial pressure of 100 Torr of H$_2$ in order to ensure recovery of the starting material after reaction. The spectrum exhibited bands with maxima at 455, 500, 590, 640 (sh), and ca. 800 nm (Figure 1b, Table 2). The position of the longest wavelength absorption has not been mapped out in full because the photomultiplier loses sensitivity rapidly beyond 800 nm. The wavelengths of the band maxima in the transient spectrum measured at 296 K are an excellent match to those from the spectrum obtained after irradiation of the dihydride precursor in a methane matrix at 12 K. The match in relative intensity is less good, notably at 490 nm (Figure 1a,b), but nevertheless, the spectrum provides unequivocal evidence that Os(dmpe)$_2$ is also formed in solution.

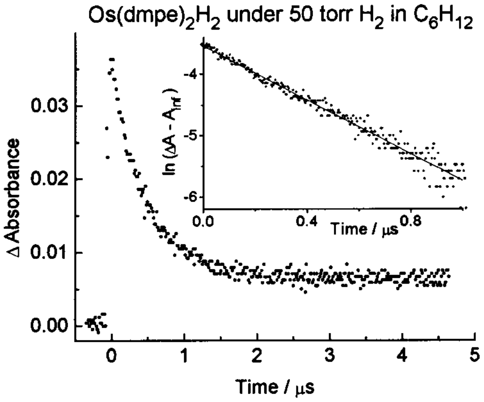

**Figure 3.** Transient kinetic trace measured after laser flash photolysis of a cyclohexane solution of Os(dmpe)$_2$H$_2$ (ca. 10$^{-3}$ mol dm$^{-3}$) under 50 Torr H$_2$ and ca. 700 Torr argon. The inset shows the corresponding first-order plot (laser wavelength 266 nm, monitoring wavelength 450 nm, average of 8 shots, no smoothing).

**Table 3. Second-Order Rate Constants for Reaction of Os(dmpe)$_2$**

| quencher | pressure/ concentration range | rate constant $k_2$/ dm$^3$ mol$^{-1}$ s$^{-1}$ |
|---|---|---|
| $H_2$ | 50−200 Torr | (7.2 ± 0.9) × 10$^9$ |
| CO | 27−155 Torr | (2.0 ± 0.6) × 10$^9$ |
| $N_2$ | 108−615 Torr | (1.2 ± 0.4) × 10$^8$ |
| $C_2H_4$ | 11−171 Torr | (1.1 ± 0.2) × 10$^8$ |
| $Et_3SiH$ | 4.3 × 10$^{-4}$ to 7.2 × 10$^{-3}$ mol dm$^{-3}$ | (1.4 ± 0.3) × 10$^8$ |

Quenching experiments were carried out to determine the rates of reaction of the transient species with different substrates. Laser flash photolysis experiments of *cis*-Os(dmpe)$_2$H$_2$ in cyclohexane were carried out under different partial pressures of H$_2$ (50−200 Torr, always made up to a total pressure of 1 atm with argon). The transient absorption was monitored at the maxima 450, 500, 590, 640, and 800 nm. The transient absorption decayed following pseudo-first-order kinetics and returned almost to the original values. The best signal-to-noise ratio was obtained at 450 nm (Figure 3), corresponding to the maximum transient absorbance. The values of the rate constants determined at wavelengths corresponding to the weaker absorption maxima were the same within experimental error. The plot of $k_{obs}$ versus concentration of hydrogen is linear (Figure 4). With the solubility of H$_2$ taken as 3.8 × 10$^{-3}$ mol dm$^{-3}$ atm$^{-1}$,[17] a value for the second-order rate constant of (7.2 ± 0.9) × 10$^9$ dm$^3$ mol$^{-1}$ s$^{-1}$ is obtained for reaction of Os(dmpe)$_2$ with hydrogen.

Similar behavior was observed when the laser flash photolysis experiments on *cis*-Os(dmpe)$_2$H$_2$ in cyclohexane were performed under pressures of CO, C$_2$H$_4$, N$_2$, and Et$_3$SiH. The resulting plots of $k_{obs}$ versus [quencher] yielded rate constants varying from ca. 10$^8$ to ca. 10$^9$ dm$^3$ mol$^{-1}$ s$^{-1}$ (Figure 4, Table 3). The very small effect of changing solvent from cyclohexane to heptane shows that Os(dmpe)$_2$ does not react with heptane

---

[16] Frequencies are measured from subtraction spectra.

[17] Wilhelm, E.; Battino, R. *Chem. Rev.* **1973**, *73*, 1. Gas solubilities in cyclohexane were taken as follows: H$_2$ (3.8 × 10$^{-3}$ mol dm$^{-3}$ atm$^{-1}$); CO (9.3 × 10$^{-3}$ mol dm$^{-3}$ atm$^{-1}$); ethene (1.4 × 10$^{-1}$ mol dm$^{-3}$ atm$^{-1}$).

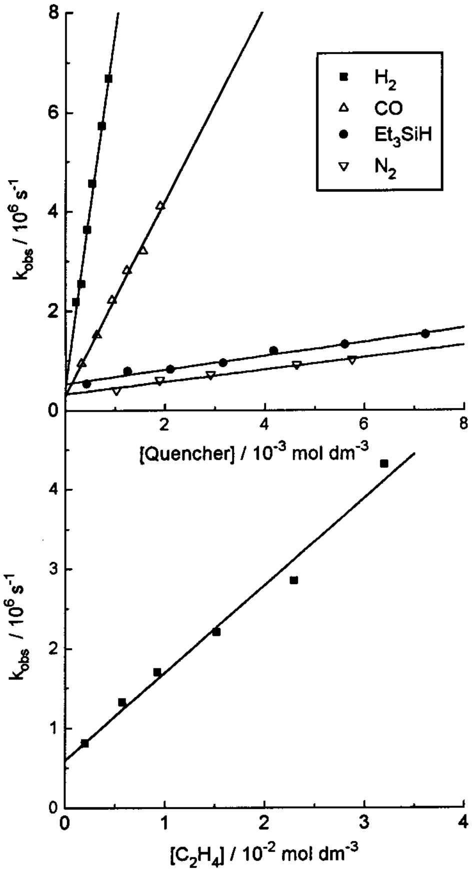

**Figure 4.** Plots showing the variation of the pseudo-first-order rate constants derived from the laser flash photolysis of Os(dmpe)$_2$H$_2$ in cyclohexane in the presence of quenching reagents (a) with H$_2$ (■), CO (△), Et$_3$SiH (●), and N$_2$ (▽); (b) with C$_2$H$_4$ (■).

preferentially, in contrast to Os(PP$_3$).[8] Indeed, there is no evidence that Os(dmpe)$_2$ reacts with alkanes.

**Steady-State Photolysis.** The photochemistry of *cis*-Os(dmpe)$_2$H$_2$ was also investigated in solution by means of NMR and IR techniques. No attempt was made to isolate the products.

**Reaction with Benzene.** The complex *cis*-Os(dmpe)$_2$H$_2$ was dissolved in a mixture of hexane/benzene (9:1) in a silica cuvette and irradiated using a Xe-arc lamp ($200 < \lambda < 400$ nm, ca. 8 h) at room temperature. The solvent was removed under vacuum, and the residue was studied by NMR in C$_6$D$_6$. The $^1$H NMR spectrum showed the resonances due to the starting material together with a new hydride signal (Table 1, conversion 35%) at $\delta$ −9.33, which appeared as a doublet of quartets, although it cannot be a first-order system (apparent $J_{HP}$ 71.4 and 20.6 Hz). The characteristic resonances of a phenyl group bound to the metal center were observed in the low-field region of the $^1$H NMR spectrum ($\delta$ 7.1−8.2 m). The $^{31}$P{$^1$H} NMR spectrum of the photoproduct displayed the pattern of an ABMQ spin system (Table 2). The resonances of the mutually trans $^{31}$P nuclei exhibited an AB pattern with a coupling constant of 264 Hz, but the remaining coupling constants were less than 20 Hz. These data suggest the formation of the *cis*-Os(dmpe)$_2$(H)(Ph).

In contrast, photolysis of a solution of Os(dmpe)$_2$H$_2$ in hexane alone resulted in precipitation. On pumping down and redissolving in C$_6$D$_6$, only starting material was observed in the $^1$H NMR spectrum. The $^{31}$P{$^1$H} NMR spectrum showed three weak singlets in addition to the precursor. Thus, photolysis under these conditions does not give rise to any tractable product.

**Reaction with Ethene.** Os(dmpe)$_2$H$_2$ was dissolved in hexane and irradiated in a quartz cuvette under 1 atm of C$_2$H$_4$ ($220 < \lambda < 485$ nm, ca. 8 h). The products were identified by means of $^1$H and $^{31}$P NMR spectra recorded in benzene-*d*$_6$. The $^1$H NMR spectrum showed two new metal hydride resonances at $\delta$ −9.47 (apparent dq, $J_{HP}$ = 68.3 and 19.7 Hz) and at $\delta$ −10.1 (quin, $J_{HP}$ = 20.0 Hz). The former, which is the major product of the photolysis, belongs to *cis*-Os(dmpe)$_2$(H)(CH=CH$_2$) and the latter is due to *trans*-Os(dmpe)$_2$(H)(CH=CH$_2$). A series of multiplets was observed between $\delta$ 8.30 and 5.68 due to the vinyl protons. With the help of broad-band phosphorus-decoupled $^1$H NMR spectra, coupling constants of vinyl protons were determined for both trans and cis isomers. The *cis*-vinyl−hydride complex exhibited three well-resolved doublets of doublets at $\delta$ 8.30, 7.26, and 6.06 with coupling constants $J_{gem}$ = 6.4, $J_{cis}$ = 12.1, and $J_{trans}$ = 18.8 Hz. Similar vinyl resonances were also observed for *trans*-Os(dmpe)$_2$(H)(C$_2$H$_3$) at $\delta$ 8.20 (dd), 6.87 (dd), and 5.68 (dd) with couplings of $J_{gem}$ = 5.3, $J_{cis}$ = 12.6, and $J_{trans}$ = 19.5 Hz. The $^{31}$P{$^1$H} NMR spectrum showed a singlet at $\delta$ 9.58 for the trans isomer and an ABMQ spin system for *cis*-vinyl−hydride complex (Table 1).

**Reaction with Et$_3$SiH.** Irradiation ($200 < \lambda < 400$ nm, ca. 5 h) of the osmium dihydride in mixtures of hexane/Et$_3$SiH (3:1) yielded a pale yellow solution. After the removal of the solvent, the residue was dissolved in benzene-*d*$_6$ and analyzed by NMR. Two new hydride resonances appeared in the high-field region of the $^1$H NMR spectrum, a broad triplet at $\delta$ −10.81 and a doublet of quartets at $\delta$ −11.26, in a 19:1 ratio. The $^{31}$P{$^1$H} NMR spectrum displayed a singlet at $\delta$ −5.13, characteristic of a trans isomer, together with multiplets at $\delta$ −0.48, −2.37, and −3.47. The lowest field resonance showed strong second-order distortions. Computer simulation of the spectrum provided the values for the coupling constants given in Table 1. The products are tentatively assigned as trans and cis isomers of Os(dmpe)$_2$(SiEt$_3$)H.

**Reaction with CO.** Finally, a hexane solution of *cis*-Os(dmpe)$_2$H$_2$ was photolyzed under 1 atm of CO for ca. 5 min, and a sample was removed for IR spectroscopy. There was no peak other than an Os−H stretching band of starting material at 1865 cm$^{-1}$. When irradiation was continued, $\nu_{CO}$ bands appeared at 2010, 1934, and 1910 cm$^{-1}$, which can probably be assigned to Os(dmpe)(CO)$_3$ (compare 2005, 1934, 1915 cm$^{-1}$ for Ru(dmpe)(CO)$_3$)[9] and another band at 1966 cm$^{-1}$. A similar experiment was performed under a $^{13}$CO atmosphere. The $\nu_{CO}$ bands of Os(dmpe)(CO)$_3$ were shifted, but no band was observed corresponding to Os(dmpe)$_2$(CO). Any monocarbonyl may have been consumed as soon as it was produced to form the osmium tricarbonyl complex.

## Discussion

The photochemistry of Os(dmpe)$_2$H$_2$ has been studied in low-temperature matrices and in solution; the solution studies include laser flash photolysis and steady-state photolysis with NMR detection. The results are

**Scheme 1. Photochemical Reactions of Os(dmpe)$_2$H$_2$ in Solution, Derived from Transient and Steady-State Experiments**

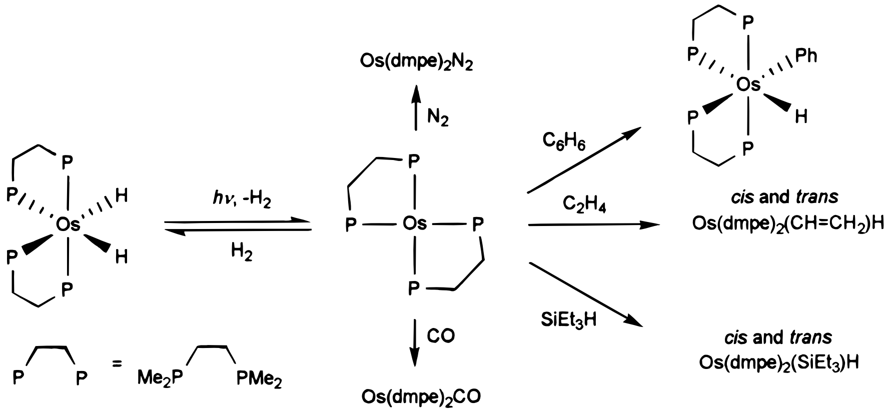

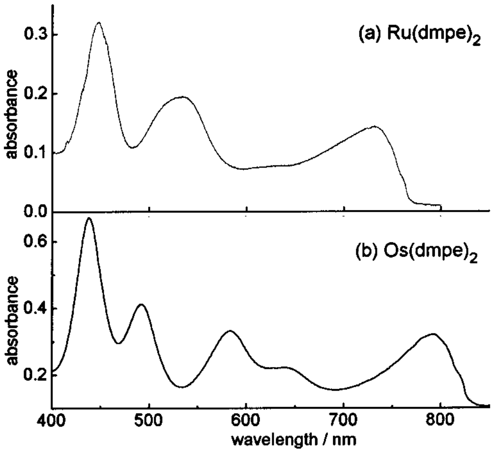

**Figure 5.** Comparison of UV−vis spectra of Ru(dmpe)$_2$ and Os(dmpe)$_2$ in methane matrices at 12 K.

fully consistent with initial photoinduced reductive elimination of $H_2$ to form Os(dmpe)$_2$. The reductive elimination is complete within the instrumental rise time of ca. 60 ns. The transient 16-electron Os(dmpe)$_2$ subsequently reacts with added reagents by oxidative addition ($H_2$, $Et_3SiH$, $C_2H_4$, $C_6H_6$) or by ligand attack (CO, $N_2$), as shown in Scheme 1. The reaction with $H_2$ re-forms the precursor. This behavior is exactly analogous to that of the ruthenium analogue, Ru(dmpe)$_2$.[4]

**Spectra and Structure.** The UV−vis spectrum of Os(dmpe)$_2$ bears a striking resemblance to that of Ru(dmpe)$_2$, as is shown in the comparison in Figure 5. Both species have a very low energy transition in the far-red end of the spectrum: that of the osmium complex (793 nm) is at even lower energy than the ruthenium complex.[4] The most intense band in each spectrum lies close to 440 nm. Between these two features, the osmium complex exhibits three further bands, while the ruthenium complex exhibits one together with a poorly resolved shoulder. We were able to determine extinction coefficients for Ru(dmpe)$_2$ in the range 1700−2400 dm$^3$ mol$^{-1}$ cm$^{-1}$.[4] Neither Os(dmpe)$_2$ nor Ru(dmpe)$_2$ shows any evidence for methane coordination since their spectra shift very little from argon to methane matrices. We have argued by comparison of the spectra of [Rh(dppe)$_2$]$^+$ with the spectra of Ru(dmpe)$_2$, Ru(depe)$_2$, and Ru(dppe)$_2$ that the Ru$^0$ complexes are square planar.[4,18] The lowest energy band has been assigned to a transition from $d_{z^2}$ to an orbital that has predominantly $p_z$ character. Three further transitions from the remaining three occupied d orbitals to $p_z$ are allowed in $D_{2h}$ symmetry, the point group for the bis-chelate. The salt of [Rh(dppe)$_2$]$^+$ has been crystallographically characterized[19] and shows a pattern of UV−vis bands similar to that of the Ru$^0$ complexes, but 10000−12000 cm$^{-1}$ to shorter wavelength. The UV−vis absorption and magnetic circular dichroism (mcd) spectra of [Rh(dppe)$_2$]$^+$ have been well investigated by Geoffroy et al.[18] Since we presented these arguments, we have completed calculations by density functional methods on Ru(PH$_3$)$_4$ and [Rh(PH$_3$)$_4$]$^+$ which predict a structure with $D_{2d}$ symmetry close to square planar and reproduce the large shift in the HOMO−LUMO gap between the neutral species and the isoelectronic cation.[10] We have also studied several related M$^0$ species that are clearly not square planar and have quite different spectra, notably, M(PP$_3$) (M = Ru, Os), Ru(CO)$_2$(PMe$_3$)$_2$(S), and Ru(CO)$_2$(dmpe)(S) (S = solvent).[7,8] We have also shown that the spectrum of Ru(dmpm)$_2$ (dmpm = Me$_2$PCH$_2$PMe$_2$) is related to that of Ru(dmpe)$_2$, but the lowest energy band is shifted to shorter wavelength (570 nm) probably as a result of the reduction in the bite angle to about 72°.[20]

The effect of moving from a second-row to a third-row element on the X-ray structures is not completely established. The structures of [Ir(PMe$_3$)$_4$]PF$_6$ and [Ir(PPh$_2$Me)$_4$]BF$_4$ show substantial $D_{2d}$ distortions from square planarity like their rhodium counterparts.[21] Unfortunately, there are no structures of analogues with chelating diphosphines except for [Ir(dppf)$_2$]BPh$_4$ and [Ir(Cy$_2$PCH$_2$CH$_2$PCy$_2$)$_2$]Cl (dppf = (bis{diphenylphosphino}ferrocene, Cy = cyclohexyl) where the ligands impose unusual steric demands forcing a nonplanar structure.[22,23] The effect of iridium on the UV−vis spectra is well illustrated by Geoffroy et al.'s study of

---

[18] Geoffroy, G. L.; Isci, H.; Litrenti, J.; Mason, W. R. *Inorg. Chem.* **1977**, *16*, 1951.

[19] The crystal structures of salts of Rh(dppe)$_2$$^+$ and Rh(dmpe)$_2$$^+$ show that both ions are close to square planar: Marder T. B.; Williams, I. D. *J. Chem. Soc., Chem. Commun.* **1987**, 1478. Hall, M. C.; Kilbourn, B. T.; Taylor, K. A. *J. Chem. Soc. (A)* **1970**, 2539.

[20] Nicasio, M. C.; Perutz, R. N. Walton, P. H. *Organometallics* **1997**, *16*, 1410

[21] Blum, O.; Calabrese, J. C.; Frolow, F.; Milstein, D. *Inorg. Chim. Acta* **1990**, *174* 149. Clark, G. R.; Skelton, B. W.; Waters, T. N.; Davies, J. E. *Acta Crystallogr. Sect. C* **1987**, *43*, 1708.

[22] Casellato, U.; Corain, B.; Graziani, R.; Longato, B.; Pilloni, G. *Inorg. Chem.* **1990**, *29*, 1193.

[23] Marder, T. B. Personal communication, unpublished structure of [Ir(Cy$_2$PCH$_2$CH$_2$PCy$_2$)$_2$]Cl.0.5 THF.

$[Rh(dppe)_2]^+$ and $[Ir(dppe)_2]^+$.[18] They showed that $[Ir(dppe)_2]^+$ exhibits bands with extinction coefficients above 1000 $dm^3\ mol^{-1}\ cm^{-1}$ at 22 800, 26 500, and 31 800 $cm^{-1}$ and showed by mcd spectroscopy that the first and last of these consist of several components. The greater number of intense components in the case of $Ir^+$ compared to $Rh^+$ is associated with important contributions from spin−orbit coupling in the third row of the transition series. Geoffroy carried out a full spin−orbit analysis, which we will not attempt to follow here since we do not have the advantage of mcd spectra. Our results make it clear that $Os(dmpe)_2$ presents an analogous situation to $[Ir(dppe)_2]^+$ and that the case for a square planar structure for $Os(dmpe)_2$ is very strong. The lowest energy band of $Os(dmpe)_2$ at 793 nm (12 600 $cm^{-1}$, methane matrix) may be assigned to the $a_g$ ($d_{z^2}$) to $b_{1u}$ ($p_z$) transition assuming $D_{2h}$ local symmetry, representing a shift 10 400 $cm^{-1}$ relative to the corresponding band of $[Ir(dppe)_2]^+Cl^-$ in acetonitrile solution.

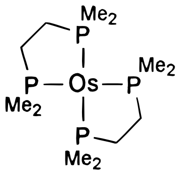

**Reactivity.** Product studies by NMR spectroscopy demonstrate that $Os(dmpe)_2H_2$ undergoes photochemical reaction with benzene, triethylsilane, and ethene to yield products expected for oxidative addition of the substrate to $Os(dmpe)_2$. However, the reactions with triethylsilane and ethene yielded products with a trans configuration in addition to the cis products expected for concerted oxidative addition. In these cases, there may also be an isomerization pathway at work.

The rate constants for reaction of $Os(dmpe)_2$ with $H_2$, CO, $C_2H_4$, and $Et_3SiH$ are very similar to those of $Ru(dmpe)_2$.[4] Unfortunately, it was not possible to measure the rate constant for reaction with benzene because of absorption by benzene at the laser wavelength. Once more, we have a demonstration that oxidative addition of $H_2$ at a square planar complex can proceed with essentially no activation barrier and with a rate constant close to the diffusion limit. The theoretical analysis of the reaction coordinate of $Ru(PH_3)_4$ with $H_2$ showed that a barrierless pathway could be achieved by initial end-on attack of $H_2$ and a gradual reorientation of the $H_2$ in the later stages of reaction.[10] At the same time one P−Ru−P angle is reduced to achieve the cis configuration of the product. This angle declines more rapidly in the later stages of reaction. No dihydrogen intermediate is predicted in this strongly exothermic process. However, the H···H distance barely starts to increase until the hydrogen has almost adopted its final orientation and is close to the final distance from the metal. The rate constant for coordination of CO at $Os(dmpe)_2$ is also close to the diffusion limit. The theoretical analysis with $Ru(PH_3)_4$ showed that the four-electron repulsion between the $d_{z^2}$ electrons and the CO $\sigma$ orbital could be avoided if the CO is tilted with respect to the normal to the $MP_4$ plane in the initial attack. At long M···CO separations the M···C−O angle is predicted to be ca. 107°.

## Conclusions

Photolysis of $Os(dmpe)_2H_2$ generates $Os(dmpe)_2$, with a square planar structure and a very rich UV−vis spectrum. This complex is the first example of a four-coordinate homoleptic $Os^0$ complex for which structural data have been obtained. This species has been characterized both in low-temperature matrices and in solution at ambient temperature, demonstrating the complementarity of matrix isolation and time-resolved spectroscopy. Like its ruthenium analogue it reacts both with hydrogen and with carbon monoxide with rate constants close to the diffusion limit.

## Experimental Section

**General Methods and Materials.** Osmium tetroxide and dmpe were purchased from Strem. $(NH_4)_2OsCl_6$ was prepared according to the literature procedure[24] or purchased directly (Strem). The synthesis of *trans*-$Os(dmpe)_2Cl_2$ followed the literature procedure except that the final treatment with hydrazine hydrate was omitted.[25] It was used without chromatographic purification. Compounds were prepared and manipulated under $O_2$-free atmospheres using standard Schlenk, high-vacuum, and glovebox techniques. Solvents for synthesis (AR grade) were dried and degassed before use, and solvents for flash photolysis experiments (Aldrich, HPLC grade) were refluxed over calcium hydride under 1 atm of argon. Benzene-$d_6$ (Goss Scientific Instruments, Ltd.) was dried by stirring over potassium/benzophenone and then transferred into NMR tubes under vacuum. Gases used for matrix isolation and flash photolysis (Ar, $CH_4$, $H_2$, $N_2$, CO, $C_2H_4$) were BOC research grade (99.999% purity). Triethylsilane was obtained from Aldrich and stored over activated 3 Å molecular sieves. NMR spectra were recorded on Bruker MSL300 or AMX500 spectrometers. The $^1H$ NMR chemical shifts were referenced to residual $C_6D_5H$ at $\delta$ 7.13. The $^{31}P\{^1H\}$ NMR chemical shifts were referenced externally to $H_3PO_4$ at $\delta = 0$. Photolysis experiments were performed in quartz cuvettes using an ILC 302UV 300 W Xe arc equipped with either UV-reflecting (240−400 nm) or visible-reflecting (400−800 nm) mirrors and water filter or with a mercury arc (HPK 125 W) with $H_2O$ and $220 < \lambda < 485$ nm filters. After irradiation, samples were pumped off and dissolved in $C_6D_6$ for NMR experiments.

**Synthesis of *cis*-$Os(dmpe)_2H_2$.** *trans*-$Os(dmpe)_2Cl_2$ (0.35 g, 0.72 mmol) was dissolved in THF (30 mL). Freshly cut Na (0.35 g) was then added to the solution, and the reaction mixture was stirred under 1 atm of $H_2$ for 48 h at room temperature. The resulting gray suspension was filtered, giving a pale yellow solution, which was pumped to dryness. The residue was extracted with hexane (30 mL) and the solvent removed under vacuum to give a colorless oil, which was purified by sublimation at 60 °C onto a liquid $N_2$-cooled finger. *cis*-$Os(dmpe)_2H_2$ was obtained as a white solid. Yield: 65%. $^1H$ NMR ($C_6D_6$, 500 MHz): $\delta$ 1.82 (virtual triplet, $^2J_{PH} + {}^4J_{PH} = 6.4$ Hz, 6H, 2 × $PCH_3{}^t$), 1.57 (d, $^2J_{PH} = 7.4$ Hz, 6H, 2 × $PCH_3{}^c$), 1.53 (m, overlap prevents integration, $CH_2$), 1.40 (virtual triplet, $^2J_{PH} + {}^4J_{PH} = 5.0$ Hz, 6H, 2 × $PCH_3{}^t$), 1.28 (m, 2H, $CH_2$), 1.20 (d, $^2J_{PH} = 6.1$ Hz, 6H, 2 × $PCH_3{}^c$), 1.05 (m, 2H, $CH_2$), 0.91, (m, 2H, $CH_2$), −11.10 (m, 2H, hydride, see Table 1). The superscripts t and c refer to the pairs of $PMe_2$ groups which are mutually trans or cis. MS (EI, *m*/*z*, relative intensity, listing for $^{232}Os$ only): 494 (6, $[M^+]$), 493 (13, $[M(^{13}C_1)^+ - H_2]$), 492 (100, $[M^+ - H_2]$). Anal. Calcd for $C_{12}H_{34}P_4Os$: C, 29.27; H, 6.96. Found: C, 29.18; H, 7.24.

**Matrix Isolation Experiments.** The matrix isolation apparatus is described elsewhere.[26] Samples for IR spectros-

---

(24) Dwyer, F. P.; Hogarth, J. W. *Inorg. Synth.* **1957**, *5*, 206.
(25) Chatt, J.; Hayter R. G. *J. Chem. Soc.* **1961**, 896.

copy alone were deposited onto a $BaF_2$ window cooled by an Air Products CS202 closed-cycle refrigerator to 12−25 K. The outer windows of the vacuum shroud were also of $BaF_2$. *cis*-$Os(dmpe)_2H_2$ was sublimed from right-angle glass tubes at 333 K at the same time as a gas stream entered the vacuum shroud. Temperatures and rates of deposition were 20 K for Ar (2 mmol $h^{-1}$) and 25 K for $CH_4$ (2 mmol $h^{-1}$). The matrices were cooled to 12 K before recording the IR spectra on a Mattson Unicam Research Series FTIR spectrometer fitted with a TGS detector and a CsI beam splitter, which was continuously purged with dry $CO_2$-free air. Spectra were recorded at 1 $cm^{-1}$ resolution with 128 scans co-averaged (25 K data points with two-times zero filling). UV−vis spectra were recorded on the same sample at the same temperature on a Perkin-Elmer Lambda 7G spectrophotometer. Matrices were photolyzed through a quartz window with an ILC 302UV Xe arc as above. Photolysis wavelengths were selected with cutoff or interference filters ($\lambda = 493$ nm bandwidth ca. 30 nm). For Ar/CO experiments, a mercury arc (HPK 125 W) equipped with water, Pyrex, and UG11 (i.e., 260−390 nm) filters was employed for UV photolysis and a cutoff filter for visible photolysis (>395 nm).

The IR spectrum of $Os(dmpe)_2H_2$ in solid argon at 10 K showed bands as follows ($\bar{\nu}/cm^{-1}$): 1896 w, 1869 m, 1862 m, 1856 m, 1433 w, 1423 w, 1420 w, 1290 w, 1285 w, 1275 w, 1272 m, 1233 w, 1117 w, 1070 w, 937 s, 930 m, 924 s, 907 w, 904 w, 886 s, 851 w, 843 w, 831 m, 789 w. In solid methane the bands of the precursor were at the following wavenumbers ($\bar{\nu}/cm^{-1}$): 1891 m, 1884 m, 1882 m, 1866 m, 1233 w, 1201 w, 1117 w, 1070 w, 937 s, 934 m, 930 m, 925 s, 908 w, 905 w, 886 s, 852 w, 844 w, 831 m, 791 w.

**Laser Flash Photolysis.** The apparatus for flash photolysis experiments has been described in detail elsewhere.[4] Briefly, a frequency-quadrupled YAG laser (Quanta-Ray GCR, output at 266 nm, pulse width ca. 10 ns, energy ca. 10 mJ per pulse) is used as the excitation source, and a pulsed Xe arc lamp is used as a monitoring source. The collected light is passed through a small monochromator to a red-sensitive photomultiplier. The spectrometer is linked to a digital oscilloscope (Tektronix TDS 520), and the system is controlled by a PC. Transient signals are usually collected as 12- or 16-shot averages with a repetition rate of 1 Hz.

Samples of $Os(dmpe)_2H_2$ for flash experiments were sublimed immediately before use and handled in the glovebox exclusively. The samples were loaded into a quartz cuvette (2 mm path length) fitted with a Young's PTFE stopcock and degassing bulb. Solvent was added via cannula under argon on a Schlenk line fitted with a diffusion pump. The sample was degassed three times by freeze−pump−thaw cycles before being back-filled to 760 Torr with the appropriate gas. Gas mixtures were made up manometrically in 1 L bulbs such that the total pressure in the cell was typically 760 Torr. Liquid quenchers were added with a microliter syringe. The absorbances of the sample were typically 0.5−1.0 at 266 nm. Decays were analyzed by linear least-squares regression methods after conversion to absorbance using in-house software or by fitting the decays using Microcal Origin software. The error bars on the second-order rate constants are quoted as 95% confidence limits.

**Acknowledgment.** The YAG laser was made available thanks to the generosity of Prof. R. E. Hester and Dr. J. N. Moore. Dr. D. Dukic and Dr. A. D. Rooney gave valuable assistance in installing it and interfacing it to the laser kinetic spectrometer. We thank Prof. T. B. Marder for telling us about unpublished results. We also acknowledge the European Commission for an HCM fellowship to M.-C.N. and EPSRC and the Scientific and Technical Research Council of Turkey for financial support.

OM9806141

---

(26) Haddleton, D. M.; McCamley, A.; Perutz, R. N. *J. Am. Chem. Soc.* **1988**, *110*, 1810.